

## Control of Vertically Coupled InGaAs/GaAs Quantum Dots with Electric Fields

G. Ortner,<sup>1,3</sup> M. Bayer,<sup>1,3</sup> Y. Lyanda-Geller,<sup>2</sup> T. L. Reinecke,<sup>2</sup> A. Kress,<sup>3</sup> J. P. Reithmaier,<sup>3</sup> and A. Forchel<sup>3</sup>

<sup>1</sup>Experimentelle Physik II, Universität Dortmund, D-44221 Dortmund, Germany

<sup>2</sup>Naval Research Laboratory, Washington D.C., 20375, USA

<sup>3</sup>Technische Physik, Universität Würzburg, Am Hubland, D-97074 Würzburg, Germany

(Received 29 October 2003; published 19 April 2005)

Controllable interactions that couple quantum dots are a key requirement in the search for scalable solid state implementations for quantum information technology. From optical studies of excitons and corresponding calculations, we demonstrate that an electric field on vertically coupled pairs of In<sub>0.6</sub>Ga<sub>0.4</sub>As/GaAs quantum dots controls the mixing of the exciton states on the two dots and also provides controllable coupling between carriers in the dots.

DOI: 10.1103/PhysRevLett.94.157401

PACS numbers: 78.67.Hc, 03.67.Lx, 71.70.Gm, 73.21.La

The interdisciplinary field of quantum information processing not only offers insight into the interface between quantum and classical behavior, but it also opens important technological opportunities ranging from encryption and quantum communication ultimately to quantum computing [1,2]. Quantum information is represented by a linear combination of two states,  $|0\rangle$  and  $|1\rangle$ , on a quantum bit (“qubit”), as  $|\varphi\rangle = \alpha|0\rangle + \beta|1\rangle$ . For systems to be scalable up to large numbers of qubits and to be integrated into conventional electronics, solid state implementations are needed, and quantum dots (QDs) with their sharp atomic-like states currently are a major focus of such investigations [3].

Quantum gates between two qubits perform the essential logic operations. From a linear combination state on one qubit  $A$ ,  $|\varphi\rangle_A = \alpha|0\rangle_A + \beta|1\rangle_A$ , a gate operation produces an entangled state of two qubits,  $A$  and  $B$ , as  $|\Psi\rangle = \gamma|0\rangle_A|0\rangle_B + \delta|1\rangle_A|1\rangle_B$ . This is done by turning on a physical interaction between the qubits [4]. The most critical need in developing quantum gate implementations is to obtain *controllable* interactions between pairs of qubits. These interactions must be coherent so that the quantum information is retained. To date, proposals for quantum gates from QDs often have involved highly demanding nanoscale fabrication to manipulate the coupling between dots [4,5].

In undoped QDs, two exciton states (ground and single exciton) can be used to represent the qubit levels. Here we demonstrate controlled coupling between exciton states in QDs with an electrical gate [6]. Our approach is illustrated in the upper left sketch of Fig. 1 where an electric field manipulates the state coupling in the two dots by bringing them into and out of resonance [7]. Excitons in “vertically coupled” self-assembled InAs/GaAs QDs have been studied earlier [8–10]. Recently evidence for the coherence of these states was obtained from anticrossings in their fine structure and diamagnetic shifts [11]. The coupling between these excitons arises from the overlap of the electron and hole ( $e, h$ ) wave functions and from Coulomb interactions between them [12]. To apply an electric field to

such a pair of coupled quantum dots (CQDs) along the direction joining them, the structures sketched in the upper right inset of Fig. 1 were fabricated.

Self-assembled In<sub>0.6</sub>Ga<sub>0.4</sub>As/GaAs QDs with nominal separations of  $d = 4, 5,$  and  $6$  nm were prepared. These QDs have smaller interdot separations, and consequently larger energy differences between their confined electronic states, than do those studied earlier [11,13]. The back gate is a conventional laser contact, and the front gate consists of two Al layers, separated from the back gate by  $\sim 0.8 \mu\text{m}$ . The first front gate layer with a thickness of  $\sim 100$  nm has small holes formed by lithography with diameters down to  $\sim 200$  nm to isolate a single pair of CQDs. To obtain a homogeneous field along the growth direction, a second, optically transparent layer with a thickness of  $\sim 5$  nm is evaporated on top of the first layer. Optical excitation and luminescence collection are done through the holes in the mask. These CQD structures were

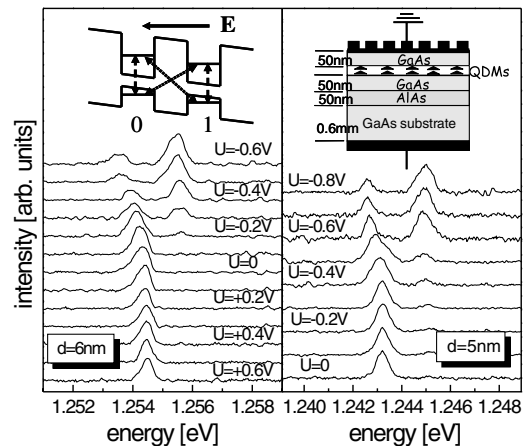


FIG. 1. PL spectra from a single In<sub>0.6</sub>Ga<sub>0.4</sub>As/GaAs CQD with 6 nm (left panel) and 5 nm separation (right panel) for varying electric field  $E$ .  $U$  is the potential applied to the structure. Left inset: Sketch of CQD structure along growth direction. Vertical (tilted) arrows indicate intradot (interdot) excitons. Right inset: Sketch of CQDs in a diode structure.

studied by photoluminescence (PL) at  $T = 2$  K with an  $\text{Ar}^+$  laser for excitation. The emission was dispersed by a double monochromator ( $f = 0.6$  m) and detected by a  $\text{LN}_2$ -cooled charge coupled device camera. Negative voltages give a reverse bias and positive voltages a forward bias. For forward bias there are leakage currents, and thus there are only small internal electric fields, and correspondingly little change in the spectra occurs.

PL spectra for a single CQD structure with 6 nm barrier are shown in Fig. 1 (left panel). At low electric field  $E$ , the spectra are dominated by a single feature that shifts to lower energies with increasing  $E$  for reverse bias. For higher fields, a second feature appears, and the lower feature becomes relatively less intense. Similar spectra for a CQD with 5 nm barrier are shown in the right panel of Fig. 1, for which the higher energy feature appears at higher voltages.

To understand these results, we consider an electron-hole pair in a CQD with an electric field  $E$  along the direction joining them, as in Fig. 1. We have calculated the orbital energies and wave functions of the four lowest exciton states  $\Psi_i$ ,  $i = 1, \dots, 4$  of one  $e, h$  pair in an  $\text{In}_{0.6}\text{Ga}_{0.4}\text{As}/\text{GaAs}$  QD pair. The theoretical approach and results for zero field are discussed in Ref. [14]. These states arise from the lowest  $s$ -like carrier states of each QD. They are obtained by diagonalizing the Hamiltonian

$$H = \begin{pmatrix} V_D^0 & t_e + V_0^e & t_h + V_0^h & V_{eh} \\ t_e + V_0^e & V_I^{10} + eEd & V_{eh} & t_h + V_1^h \\ t_h + V_0^h & V_{eh} & V_I^{01} - eEd & t_e + V_1^e \\ V_{eh} & t_h + V_1^h & t_e + V_1^e & V_D^1 \end{pmatrix} \quad (1)$$

in the basis  $|0,0\rangle$ ,  $|1,0\rangle$ ,  $|0,1\rangle$ ,  $|1,1\rangle$  that give the four possible locations of the  $e$  and  $h$  in the CQD structure [15]. The first index indicates that an electron is in the (0) dot or in the (1) dot, and the second index does the same for the hole.  $t_e(t_h)$  are the tunneling amplitudes for an  $e(h)$  between the dots. The  $V$ 's are the Coulomb interaction matrix elements involving the  $e, h$  pair [16], which depend on  $d$ .  $eEd$  is the potential drop over the distance  $d$  between dots. The calculations are made using cylindrical  $\text{In}_{0.6}\text{Ga}_{0.4}\text{As}/\text{GaAs}$  QDs of height 3 nm with finite vertical potential offsets [17]. The  $e(h)$  states are calculated adiabatically [18], which gives parabolic effective potentials in the lateral direction, and the matrix elements in Eq. (1) were calculated from them. We find that electric field dependences discussed here are not sensitively dependent on the parameter choices.

The energies are shown as functions of  $E$  in Fig. 2, and the wave functions of the two lowest exciton states  $\Psi_1$  and  $\Psi_2$  at  $E = 0$  are shown in the upper panels of Fig. 3 as functions of the  $e, h$  coordinates in the vertical direction. The wave functions spread over the two dots and are composed of  $|0,0\rangle$  and  $|1,1\rangle$  intradot and of  $|1,0\rangle$  and

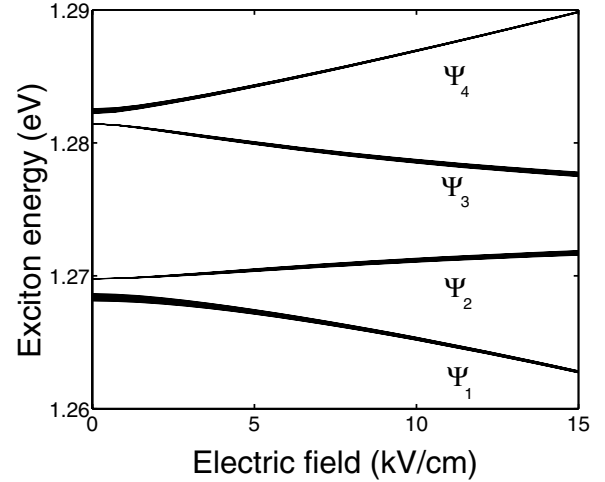


FIG. 2. Calculated energies of four lowest lying exciton states of  $\text{In}_{0.6}\text{Ga}_{0.4}\text{As}/\text{GaAs}$  CQDs with 6 nm separation vs electric field  $E$ . Widths of lines are proportional to transition oscillator strengths.

$|0,1\rangle$  interdot excitons. The relative amplitudes of the features in each wave function are determined by  $V_D^i - V_I^{ij}$ ,  $t_e$  and  $t_h$ . The line widths in Fig. 2 are proportional to the exciton oscillator strengths, which are given by the probability of  $e$  and  $h$  being at the same position, i.e., by the wave function amplitude at  $\mathbf{r}_e = \mathbf{r}_h$ . For  $E = 0$ ,  $\Psi_1$  and  $\Psi_4$  are orbitally symmetric and optically bright, and  $\Psi_2$  and  $\Psi_3$  are orbitally antisymmetric and dark, as can be seen for  $\Psi_1$  and  $\Psi_2$  in Fig. 3.

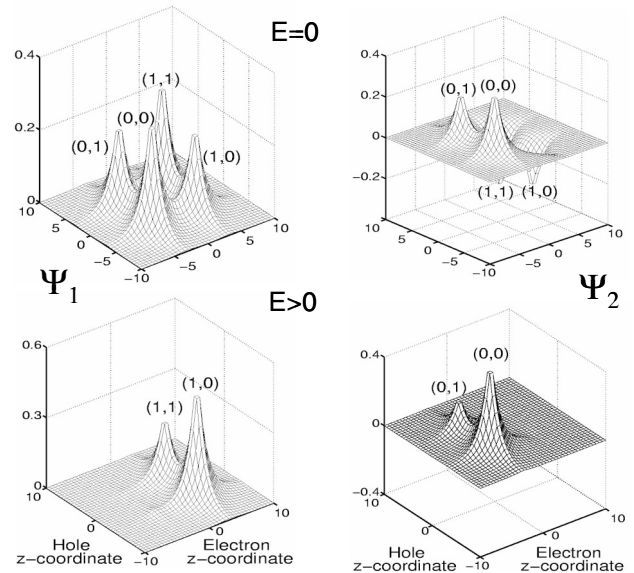


FIG. 3. Calculated wave functions of the lowest two exciton states in  $\text{In}_{0.6}\text{Ga}_{0.4}\text{As}/\text{GaAs}$  CQDs as functions of electron and hole coordinates along the axis joining the dots. Electric field  $E = 0$  is given in the upper panels and  $E = 6.4$  kV/cm (representing a potential of 0.6 V) is given in the lower panels. The dots are located at  $\pm 3$  nm along the growth direction.

The experimental electric field dependences in Fig. 1 are accounted for by the two lowest states  $\Psi_1$  and  $\Psi_2$  in Fig. 2. When an electric field is applied, the intradot and interdot components of  $\Psi_1$  and  $\Psi_2$  become increasingly decoupled (lower panels in Fig. 3). For increasing field,  $\Psi_1$  moves to lower energy, becomes less intense and approaches a decoupled, optically inactive interdot exciton  $|1, 0\rangle$ .  $\Psi_2$  becomes more intense with increasing field as it approaches an optically active intradot exciton  $|0, 0\rangle$  [19].

Figure 4 gives the observed positions of the two spectral features for three different dot separations versus voltage. The qualitative behavior of the different samples is similar, with a second spectral feature appearing only for increasing field. The higher energy feature appears at higher electric field for smaller dot separations, as expected, because higher fields are required to overcome the greater tunneling for closer dots. Further, the energy splitting between  $\Psi_1$  and  $\Psi_2$  increases in going to narrower barriers. The symbols in the inset of Fig. 4 give the fields for the onset of the second spectral feature vs dot separation, which have been determined from results from several QDs for each  $d$ . The data are in good agreement with the calculations shown by the line.

In order to verify that the higher lying spectral line appearing in Fig. 1 cannot be attributed to charged exciton emission, we have also done studies in magnetic fields along the symmetry axis. Figure 5 shows spectra for bias  $U = 0$  (left panel) and for  $U = -0.4$  V (right panel) for varying magnetic fields. For  $U = 0$  a doublet splitting is observed for the single line in Fig. 1, and it has a splitting of 1.3 meV at 8 T. For  $U = -0.4$  V, the spin splitting of the lower line is 1.1 meV at 8 T. The higher energy line

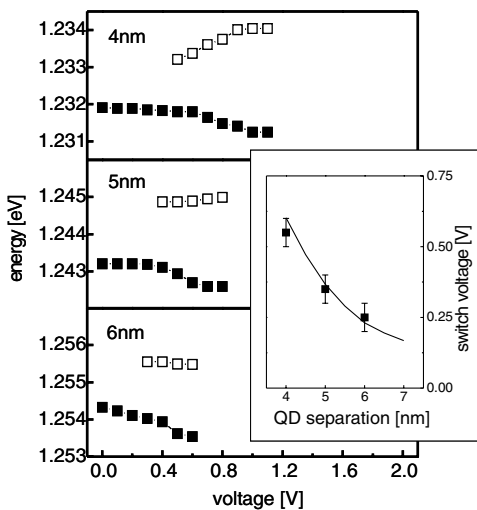


FIG. 4. Experimental results for positions of spectral features vs electric field for CQDs with separations of 4, 5 and 6 nm. The right panel gives experiment and calculations (solid line) of the electric field for onset of second spectral feature. In the calculations the upper line was taken to appear at a field for which its intensity rises to 20% of the lower line intensity.

shows a splitting of 1.7 meV. The spin splitting should be the same for a neutral and for a charged exciton because for both the splitting is determined by the  $g$  factors of the recombining electron and hole only with a total angular momentum  $M = \pm 1$  [20]. Because the higher and lower lying lines have different splittings at the same  $U$ , the upper line should not be attributed to charged exciton recombination. The difference between the  $g$  factors of the low energy lines for  $U = 0$  and  $-0.4$  V comes from the distortion of exciton wave function by the electric field. On the other hand,  $\Psi_1$  and  $\Psi_2$ , have different orbital functions at the nonzero field and therefore have different  $g$  factors, consistent with the observations.

We also note that the picture of the exciton states given here is consistent with the diamagnetic shifts of the spectral lines in Fig. 1. The inset of Fig. 5 gives the diamagnetic shifts of the  $U = 0$  and  $-0.4$  V lines for QDs separated by 6 nm. The shift of the  $U = 0$  line is to a good approximation equal to half the sum of the shifts of the two lines at  $-0.4$  V, which is in accord with our calculations within a few percent. The basic physics can be seen by noting that at high electric field the states  $\Psi_1$  and  $\Psi_2$  are approximately an intradot and an interdot exciton with corresponding diamagnetic shifts. For the present QDs for which the tunneling energies ( $t_e + t_h$ ) exceed the Coulomb energies ( $V_D^i - V_I^j$ ), at  $U = 0$   $\Psi_1$  is  $\approx 0.5(|0, 0\rangle + |0, 1\rangle + |1, 0\rangle + |1, 1\rangle)$  for which the diamagnetic shift is half the sum of the shifts of an interdot and an intradot exciton.

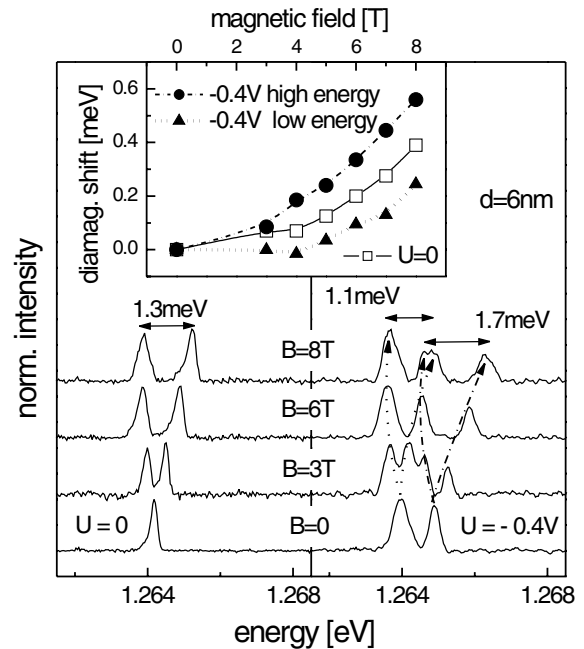


FIG. 5. PL spectra of an  $\text{In}_{0.6}\text{Ga}_{0.4}\text{As}/\text{GaAs}$  CQD for varying magnetic fields oriented along the molecule axis. The left (right) panel shows data for  $U = 0$  ( $U = -0.4$  V). The inset gives measured diamagnetic shifts of the emission lines at  $U = 0$  and  $U = -0.4$  V for an  $\text{In}_{0.6}\text{Ga}_{0.4}\text{As}/\text{GaAs}$  CQD with 6 nm separation.

In summary, we have demonstrated control of the hybridization of electron-hole pair states in CQDs with an electric field, which comes mainly from modifying the relative energies of the two QDs with the field. The tunnel and Coulomb interactions, which determine the coupling, control the entanglement of qubit gates in several systems: (i) If two excitons are introduced into a CQD structure by coherent optical techniques, electric field pulses would control the entanglement between them. (ii) The two Zeeman levels of an excess carrier spin also provide an attractive representation of a qubit in part because of evidence that their dephasing times are long [21]. The interactions between two spin qubits as well as those for two exciton qubits result from carrier tunneling between dots and Coulomb interactions, and they are described by the parameters obtained here. (iii) In addition, quantum gates between the electron and hole states in a pair of QDs have also been advanced [22] in which case entanglement can be obtained directly from the present work on excitons. Finally we note that (i) the electric field dependences of the spectra, (ii) the diamagnetic shifts of the two spectral features, and (iii) the systematic dependences of these features on separation all are consistent with quantum mechanical, coherent coupling between the dots studied here.

Support by the DARPA QuIST program, the Deutsche Forschungs-gemeinschaft, the Office of Naval Research, and the ONR Nanoscale Electronics Program is acknowledged.

- 
- [1] See, e.g., *The Physics of Quantum Information*, edited by D. Bouwmeester, A. Ekert, and A. Zeilinger (Springer, Berlin, 2000).
- [2] L. K. Grover, Phys. Rev. Lett. **79**, 325 (1997); P. W. Shor, *Proceedings of 35 Annual Symposium of Foundations of Computer Science, Santa Fe, NM*, edited by S. Goldwasser (IEEE Computer Society Press, Los Alamitos, 1994), p. 124.
- [3] X. Q. Li *et al.*, Science **301**, 809 (2003); A. Zrenner *et al.*, Nature (London) **418**, 612 (2002), and references therein.
- [4] D. Loss and D. P. DiVincenzo, Phys. Rev. A **57**, 120 (1998).
- [5] B. Kane, Nature (London) **393**, 133 (1998).
- [6] Model results for electrical gates on CQDs have been discussed in G. Burkard *et al.*, Phys. Rev. B **62**, 2581 (2000); electric field control of CQDs has been studied in I. Shtrichman *et al.*, Phys. Rev. B **65**, 081303 (2002), but evidence for coherent coupling was not obtained there.
- [7] Coherent coupling for pairs of quantum wells has been studied previously, including the onset of THz emission due to tunneling. See, for example, J. Shah, *Ultrafast Spectroscopy of Semiconductors and Semiconductor Nanostructures* (Springer, New York, 1999), Chapt. 2.
- [8] M. Bayer *et al.*, Science **291**, 451 (2001).
- [9] The detailed structures of vertical CQDs are not yet known well. Other PL data interpretations are possible such as dot coupled to the wetting layer of other dot.
- [10] Interactions between QDs in systems based on gated quantum wells also have been seen, but their coupling typically is small  $\sim 1$  meV.
- [11] G. Ortner *et al.*, Phys. Rev. Lett. **90**, 086404 (2003).
- [12] The dephasing of excitons in single QDs has been studied in P. Borri *et al.*, Phys. Rev. Lett. **87**, 157401 (2001); and compared to that in CQDs in **91**, 267401 (2003).
- [13] Anticrossings among the fine structure spin split exciton states  $\Psi_1$  and  $\Psi_2$  in magnetic fields were studied in Ref. [11] to demonstrate coherent coupling between the dots. For those studies InAs/GaAs coupled dots with large interdot separations of 7–8 nm were used, which gave small splittings ( $\sim 1$  meV) between their confined orbital states  $\Psi_1$  and  $\Psi_2$ . In this way the magnetic field energies could become comparable to the differences between the orbital energies. In<sub>0.6</sub>Ga<sub>0.4</sub>As/GaAs structures with smaller interdot separations (4–6 nm), which gave larger orbital splittings between  $\Psi_1$  and  $\Psi_2$ , were studied in the present work using electric fields. Because of the larger orbital splittings, multiple resonances between the spin states of  $\Psi_1$  and  $\Psi_2$  could not occur for the available magnetic field range. In Ref. [8] the barrier width dependence of the splitting between orbital states  $\Psi_1$  and  $\Psi_4$  was studied. Splittings up to several 10's of meV were observed, in agreement with calculations such as Fig. 2.
- [14] Y. Lyanda-Geller *et al.*, Phys. Rev. B **69**, 161308 (2004).
- [15] The basis functions  $|\dots\rangle$  in Eq. (1) are products of orthonormalized single electron and hole states for isolated dots that include the effect of the other's potential [14].
- [16] In terms of single particle electron (hole) wave functions  $\psi_{i,(j)}(\mathbf{r}_{e,(h)})$  on dots  $i, j = 0, 1$ , the Coulomb matrix elements are  $V_I^{i,j} = \langle \psi_i(\mathbf{r}_e) \psi_j(\mathbf{r}_h) | H_{eh} | \psi_i(\mathbf{r}_e) \psi_j(\mathbf{r}_h) \rangle$ ,  $V_D^i = V_I^{ii}$ ,  $V_{eh} = \langle \psi_i(\mathbf{r}_e) \psi_{j(i)}(\mathbf{r}_h) | H_{eh} | \psi_j(\mathbf{r}_e) \psi_{i(j)}(\mathbf{r}_h) \rangle$ , and  $V_i^{e(h)} = \langle \psi_i(\mathbf{r}_e) \psi_i(\mathbf{r}_h) | H_{eh} | \psi_{j(i)}(\mathbf{r}_e) \psi_{i(j)}(\mathbf{r}_h) \rangle$  where  $H_{eh}$  is the  $e$ - $h$  Coulomb interaction [14].
- [17] The parameters were obtained from C. Pryor, Phys. Rev. B **60**, 2869 (1999), using interpolations for 60% In concentration. Potential offset in growth direction for electrons and holes were 0.35 and 0.07 eV respectively; the lateral potentials were taken to be parabolic with quantization energies of 20 meV for electrons and holes; the masses in lateral direction for both electrons and holes were 0.038 and those in growth direction were 0.06 and 0.4 for electrons and holes, respectively.
- [18] M. Korkusinski and P. Hawrylak, Phys. Rev. B **63**, 195311 (2001).
- [19] Examples of CQDs have also been studied in which the energies of the two individual QDs are different at  $E = 0$  and are brought into resonance with a field.
- [20] See, e.g., F. Findeis *et al.*, Phys. Rev. B **63**, 121309 (2001).
- [21] J. A. Gupta *et al.*, Phys. Rev. B **59**, R10421 (1999); T. Fujisawa *et al.*, Phys. Rev. B **63**, 081304 (2001); J. M. Elzerman *et al.*, Nature (London) **430**, 431 (2004); M. Kroutvar *et al.*, Nature (London) 431 (to be published).
- [22] See, e.g., P. Hawrylak *et al.*, Condensed Matter News **7**, 16 (1999).